Integral Test of JENDL-3.3 with Shielding Benchmarks

Naoki YAMANO[*†]

[*] *Shielding Integral Test Working Group, Japanese Nuclear Data Committee*

[†] *Department of Nuclear Design, Sumitomo Atomic Energy Industries, Ltd.,*

2-10-14 Ryogoku, Sumida-ku, Tokyo 130-0026, Japan

e-mail: yamano@sae.co.jp

Integral tests of neutron and gamma-ray production data for cross-section libraries based on the Japanese Evaluated Nuclear Data Library, Version 3.3 (JENDL-3.3) have been performed by using shielding benchmarks. An evaluation scheme for shielding benchmark analysis established in Japanese Nuclear Data Committee (JNDC) was applied to the integral test for medium-heavy nuclei such as Oxygen, Sodium, Aluminum, Silicon, Titanium, Vanadium, Chromium, Iron, Cobalt, Nickel, Copper, Zirconium, Niobium, Molybdenum, Tungsten and Mercury. Calculations were made based on a continuous-energy Monte Carlo code MCNP4C and multi-group discrete ordinates codes ANISN, DORT and TORT. Calculations with JENDL-3.2, ENDF/B-VI, EFF-2, FENDL-1 and FENDL-2 were also made for comparison. The results of JENDL-3.3 were generally satisfactory and the cross-section libraries generated with JENDL-3.3 were verified to shielding applications for fission and fusion reactors.

1. Introduction

The latest Japanese Evaluated Nuclear Data Library, Version 3.3 (JENDL-3.3) was released on May 2002. The Shielding Integral Test Working Group in the Japanese Nuclear Data Committee (JNDC) has been in charge of verification work for JENDL-3.3 through shielding benchmark tests. Recently, a point-wise cross-section library, FSXLIB-J33, and a multi-group library, MATXS-J33 were produced by Japan Atomic Energy Research Institute (JAERI) and Sumitomo Atomic Energy (SAE).[1)] In order to verify the cross-section libraries based on JENDL-3.3, integral tests with shielding benchmarks have been performed for medium-heavy nuclei such as Oxygen, Sodium, Aluminum, Silicon, Titanium, Vanadium, Chromium, Iron, Cobalt, Nickel, Copper, Zirconium, Niobium, Molybdenum, Tungsten and Mercury. An evaluation scheme[2)] established in JNDC was adopted in the present study.

2. Evaluation Scheme

For the integral test of cross sections by using shielding benchmarks, we should select appropriate integral measurements of different types. In the present study, we selected a number of spectrum measurements listed in **Table 1** that were characterized as having high sensitivity to the nuclear data of interest. For calculation, we used a continuous-energy Monte Carlo code MCNP4C[3)] and multi-group discrete ordinates codes ANISN[4)], DORT[5)] and TORT[6)]. A systematic analysis procedure was introduced to specify the accuracy and definite problems for typical reactions of nuclear data when discrepancy was found between calculation result and measurement. Calculations with JENDL-3.2[7)], ENDF/B-VI[8)], EFF-2[9)], FENDL-1[10)] and FENDL-2[11)] were also made for comparison.

3. Results and Discussions

1. Oxygen

A JAERI-FNS benchmark result for liquid oxygen measured at 0 degree from 20 cm penetration is shown in **Fig. 1**. The neutron spectrum calculated with JENDL-3.3 shows a good agreement with experiment, and it is improved compared with JENDL-3.2. Gamma-ray spectrum measurement at FNS for $LiAlO_2$ is shown in **Fig. 2**. The gamma-ray peaks from discrete inelastic reactions are well reproduced with JENDL-3.3, while a peak around at 6 MeV is missing in JENDL-3.2.

---

[*] C. Ichihara (KURRI), K. Ueki (NMRI), Y. Matsumoto (MES), F. Maekawa (JAERI), C. Konno (JAERI), Y. Hoshiai (CRC), K. Sasaki (ARTECH), M. Takemura (KHI), T. Nishitani (JAERI), O. Sato (JAERI), S. Maeda (JNC), M. Kawai (KEK), A. Hasegawa (JAERI)

2. Sodium

For thick neutron penetration problems, JASPER IVFS-IC/Pb.9 and IHX-IB/Pb benchmarks are shown in **Figs. 3** and **4**, respectively. The results with JENDL-3.3 indicate a good agreement with both measurements, while results with ENDF/B-VI show overestimation compared with experiments in the energy range below 1.5 MeV. The difference is attributed to inelastic reactions based on the sensitivity analysis.

3. Iron

For relatively thin neutron transmission benchmarks, we selected KfK and NIST experiments from iron spheres with a ^{252}Cf source in the center. The result is shown in **Fig. 5** for the KfK iron sphere of 40 cm in diameter. Neutron spectrum calculated with MCNP4C shows good agreement except for resonance minima below 400 keV, but a good agreement is generally obtained between calculation and measurement. **Figure 6** shows the result of the NIST iron sphere of 50.7 cm in diameter. The result with JENDL-3.3 is similar to that with JENDL-3.2, however JENDL-3.3 indicates slightly larger than that of ENDF/B-VI in the energy range between 1.6 and 2 MeV. This tendency also appears in the KfK benchmark.

For relatively thick neutron penetration benchmarks, we adopted ASPIS and FNS experiments. **Figure 7** shows comparison between calculated results and the ASPIS measurement at 113.98-cm depth of iron slabs. **Figure 8** indicates comparisons between calculated results with MCNP4C/DORT and the FNS measurement at 81-cm depth of large iron cylinder. In these benchmarks, neutron fluxes calculated with JENDL-3.3 in the energy range between 0.7 and 1 MeV are slightly underestimated compared with experiments. On the contrary, results with ENDF/B-VI are much better in this energy region. Two calculation results with DORT and MCNP4C show the same flux profile, so that we recommend improvement should be made in the energy range. For lower energy region below the 24 keV s-wave resonance, JENDL-3.3 slightly indicates overestimation compared with measurement as shown in **Fig. 8**. The calculation to experimental (C/E) ratio integrated over between 1 and 1000 eV is relatively large for JENDL-3.3, whereas the C/E deviations with JENDL-3.3 at each measured position are relatively smaller than those with another libraries.

For gamma-ray production benchmarks, we employed KfK and FNS measurements. The results with JENDL-3.3 indicate good agreement with measurements as shown in **Figs. 9** and **10**, and the results are better than those with JENDL-3.2.

3. Vanadium

Figures 11 and **12** show neutron and gamma ray benchmarks performed by FNS, respectively. Neutron flux calculated with JENDL-3.3 shows underestimation below 1 keV, while it makes better compared with JENDL-3.2 as shown in **Fig. 11**. In the energy region above 20 keV, a good agreement is generally obtained except between 0.1 and 1 MeV. For gamma-ray production data, JENDL-3.3 is improved from JENDL-3.2 as shown in **Fig. 12**.

4. Tungsten

Neutron flux measurements of FNS and OKTAVIAN are shown in **Figs. 13** and **14**, respectively. Neutron spectrum above 150 keV is slightly underestimated compared with the FNS experiment. For leakage gamma-ray measurements of FNS and OKTAVIAN, the profile of photon flux is generally acceptable compared with JENDL-3.2 as shown in **Figs. 15** and **16**.

5. Mercury

Neutron flux measurement of FNS is shown in **Fig. 17**. Neutron spectra at thickness of 7 and 14 cm are generally acceptable while the calculated values slightly show underestimation. Gamma-ray heating rate measurement of FNS indicates underestimation as shown in **Fig. 18**.

6. Titanium and Niobium

Neutron flux measurements of OKATVIAN for Titanium and Niobium are shown in **Figs. 19** and **20**, respectively. Neutron spectra show overestimation below 1 MeV. Gamma-ray spectra for Titanium and Niobium are generally acceptable as shown in **Figs. 21** and **22**, respectively.

7. Aluminum, Silicon, Chromium, Cobalt, Nickel, Copper, Zirconium and Molybdenum

Figures 23 and **24** show the comparisons between calculation and measurement for FNS and OKTAVIAN Copper experiments, respectively. The results of JENDL-3.3 are in good agreement with experiments except below 1 keV for the FNS benchmark. Comparisons of neutron fluxes between calculations and measurements for Aluminum, Silicon, Chromium, Cobalt, Nickel, Zirconium and Molybdenum are similar results to those of JENDL-3.2.

4. Conclusion

Integral tests with the FSXLIB-J33 and the MATXS-J33 libraries based on JENDL-3.3 have been performed for Oxygen, Sodium, Aluminum, Silicon, Titanium, Vanadium, Chromium, Iron, Cobalt, Nickel, Copper,

Zirconium, Niobium, Molybdenum, Tungsten and Mercury for various shielding benchmarks. The results were generally satisfactory and the new libraries would be acceptable for shielding applications for fission and fusion reactors. However, some problems in JENDL-3.3 remained, and the improvement should be made in the next release of JENDL.

Acknowledgments

Authors are indebted to M. Wada of Startcom Co. Ltd. for his calculations of the FNS benchmarks. The work was performed as an activity of the Shielding Integral Test Working Group of JNDC.

References

1) K. Kosako, C. Konno, T. Fukahori, K. Shibata, "MCNP and MATXS Cross Section Libraries Based on JENDL-3.3," to be presented in this Symposium (2002).
2) N. Yamano, "On the Integral Test Method for Neutron Nuclear Data Evaluation," *Ann. Nucl. Energy*, **24**, 1085 (1997).
3) J.F. Briesmeister, (Ed.), "MCNP-A General Monte Carlo N-Particle Transport Code, Version 4C," LA-13709-M (2000).
4) W.W. Engle Jr., "A USER'S MANUAL FOR ANISN: A One Dimensional Discrete Ordinates Transport Code with Anisotropic Scattering," K-1693 (1967).
5) W.A. Rhodes, R.L. Childs, "The DORT Two-Dimensional Discrete Ordinates Transport Code," *Nucl. Sci. Eng.*, **99**, 88 (1988).
6) W.A. Rhoades, D.B. Simpson, "The TORT Three-Dimensional Discrete Ordinates Neutron/Photon Transport Code (TORT Version 3)," ORNL/TM-13221 (1998).
7) T. Nakagawa, K. Shibata, S. Chiba, et al., "Japanese evaluated nuclear data library version 3 revision-2: JENDL-3.2," *J. Nucl. Sci. Technol.*, **32**, 1259 (1995).
8) P.F. Rose, (Ed.), "ENDF-201 ENDF/B-VI Summary Documentation," BNL-NCS-17541 (1991).
9) H.D. Lemmel, et al., IAEA-NDS-170 (1995).
10) S. Ganesan, P.K. McLaughin, "FENDL/E Evaluated Nuclear Data Library of Neutron Nuclear Interaction Cross-Sections and Photon Production Cross-Sections and Photon-Atom Interaction Cross Sections for Fusion Applications Version 1.0 of May 1994," IAEA-NDS-128 (1995).
11) A.B. Pashchenko, et al., "FENDL-2: An Improved Nuclear Data Library for Fusion Applications," *Proc. Int. Conf. on Nuclear Data for Science and Technology*, Trieste, Italy, 19-24 May 1997, Vol. 59, Part II, p.1150 (1997).
12) N. Yamano, et al., *J. Nucl. Sci. Technol., Supplement 2*, pp. 841-846 (2002).

Table 1 Shielding Benchmark Experiments for Integral Test of JENDL-3.3*

Nuclide	Benchmark Experiments
Oxygen	FNS
Sodium	SDT4, SDT12, JASPER (IVFS-IC/Pb.9, IHX-IB/Pb)
Aluminum	OKTAVIAN, IPPE
Silicon	OKTAVIAN
Titanium	OKTAVIAN
Vanadium	FNS
Chromium	OKTAVIAN
Iron	SDT1, SDT11, FNS, ASPIS, KfK, NIST
Cobalt-59	OKTAVIAN
Nickel (include SS)	IPPE, ORNL, FNS
Copper	OKTAVIAN, FNS
Zirconium	OKTAVIAN
Niobium	OKTAVIAN
Molybdenum	OTRAVIAN
Tungsten	OKTAVIAN, FNS
Mercury	FNS

* Benchmarks adopted in this study are referred in elsewhere.[12)]

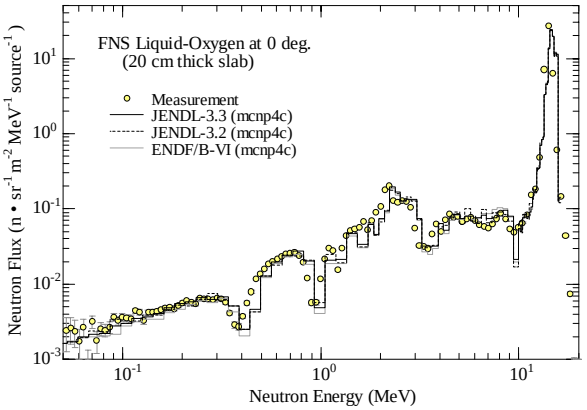

Fig. 1 Results of FNS Oxygen benchmark.

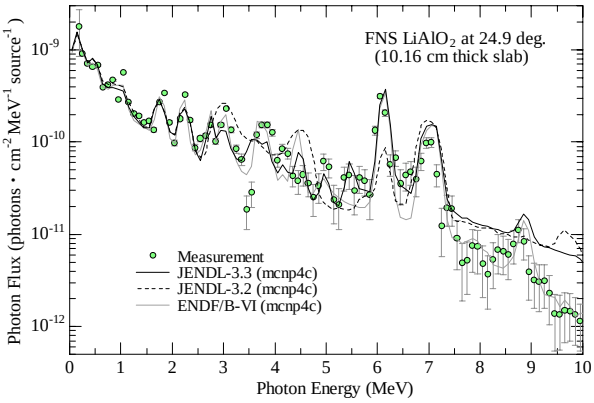

Fig. 2 Results of FNS $LiAlO_2$ benchmark.

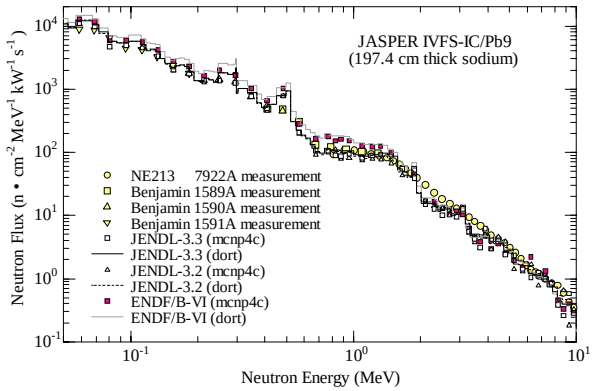

Fig. 3 Results of JASPER IVFS-IC/Pb benchmark.

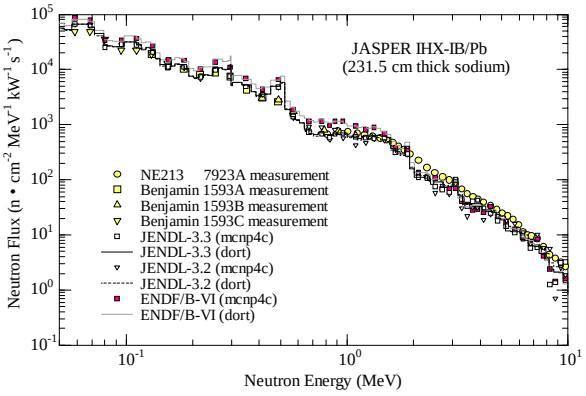

Fig. 4 Results of JASPER IHX-IB/Pb benchmark.

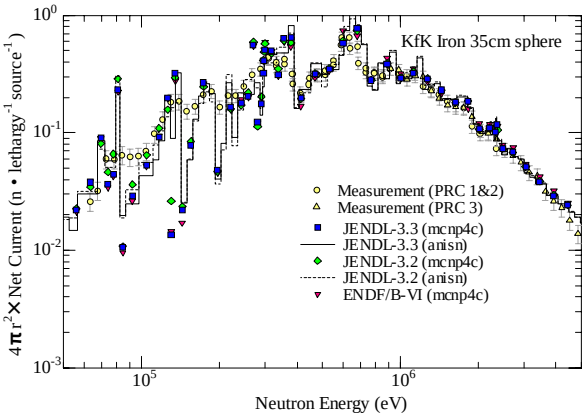

Fig. 5 Results of KfK Iron benchmark.

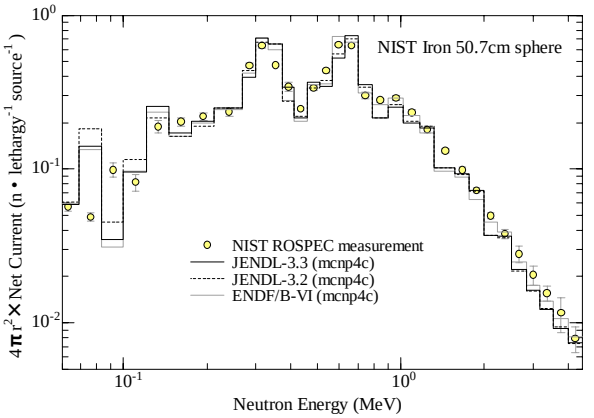

Fig. 6 Results of NIST Iron benchmark.

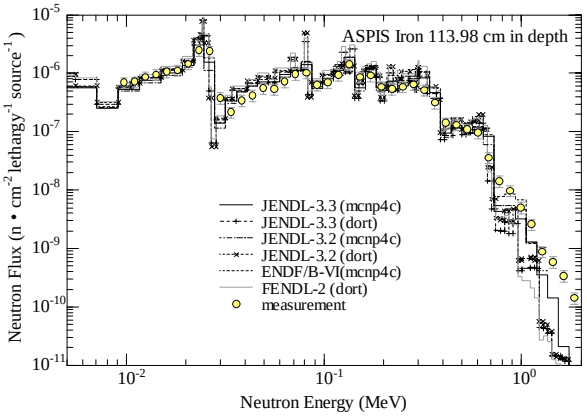

Fig. 7 Results of ASPIS Iron benchmark.

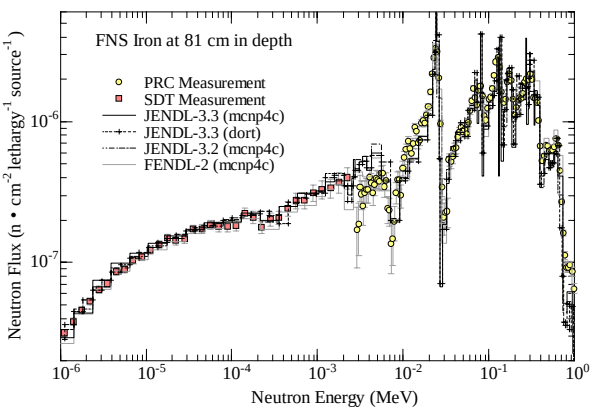

Fig. 8 Results of FNS Iron benchmark.

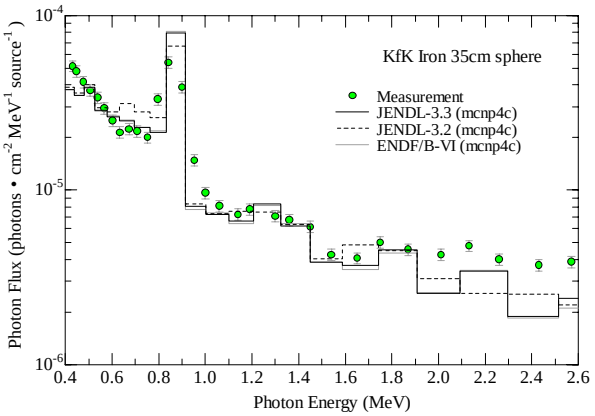

Fig. 9 Results of KfK Iron benchmark.

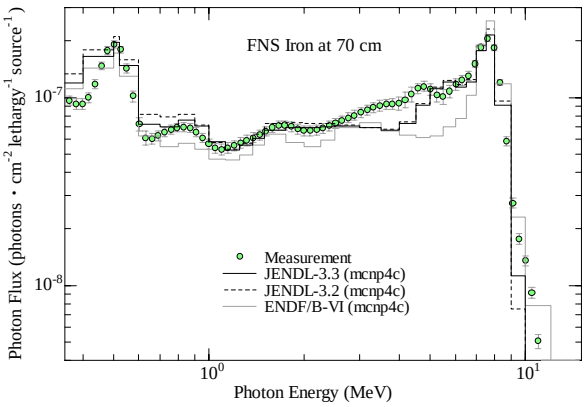

Fig. 10 Results of FNS Iron benchmark.

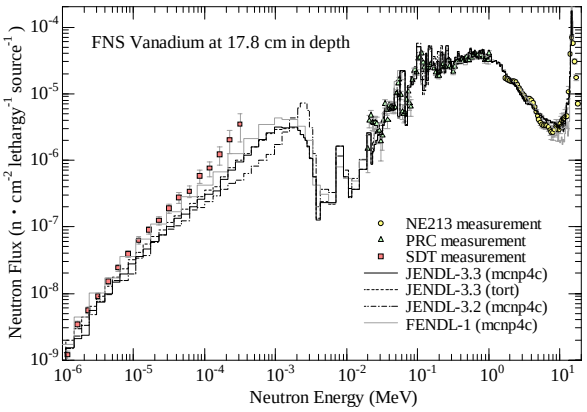

Fig. 11 Results of FNS Vanadium benchmark.

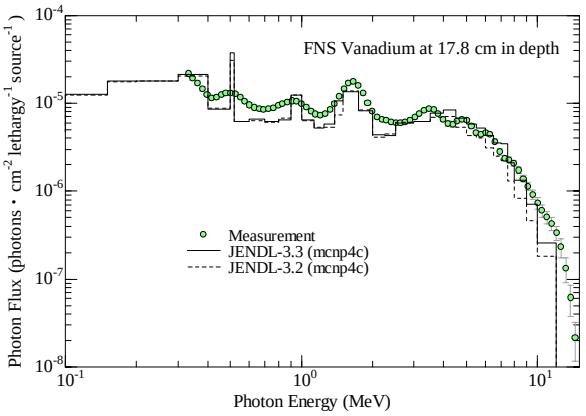

Fig. 12 Results of FNS Vanadium benchmark.

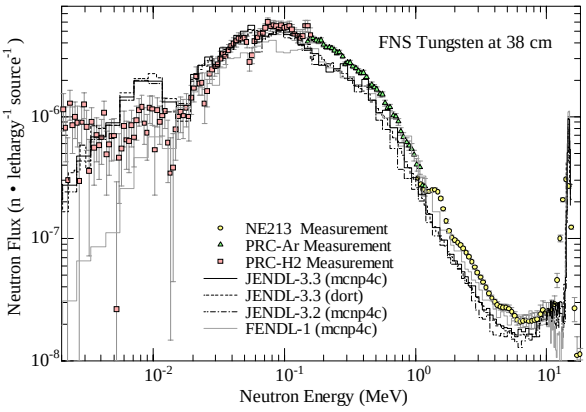

Fig. 13 Results of FNS Tungsten benchmark.

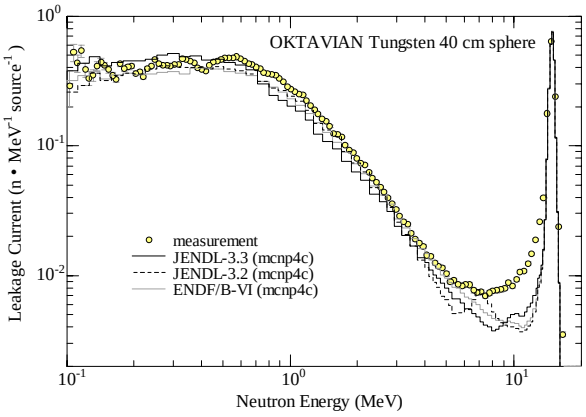

Fig. 14 Results of OKTAVIAN Tungsten benchmark.

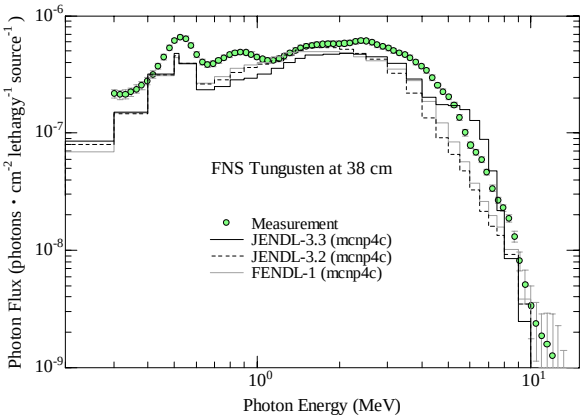

Fig. 15 Results of FNS Tungsten benchmark.

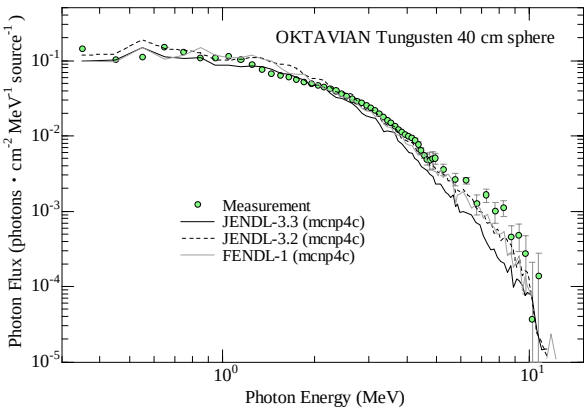

Fig. 16 Results of OKTAVIAN Tungsten benchmark.

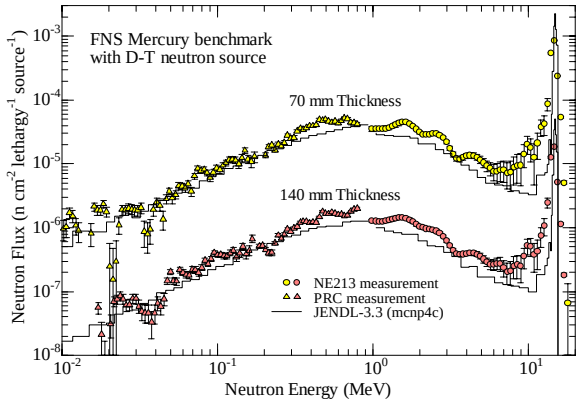

Fig. 17 Results of FNS Mercury benchmark.

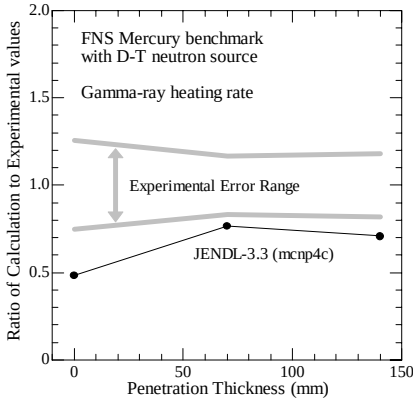

Fig. 18 Results of FNS Mercury benchmark.

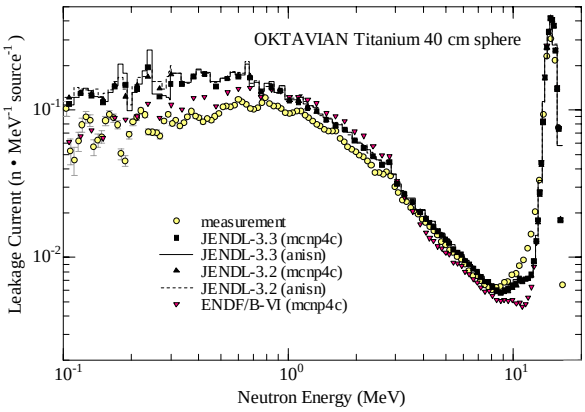

Fig. 19 Results of OKTAVIAN Titanium benchmark.

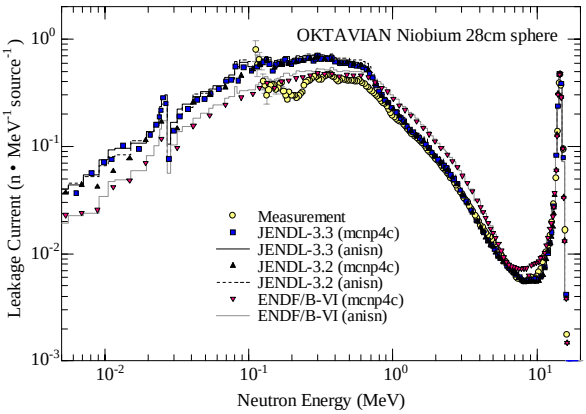

Fig. 20 Results of OKTAVIAN Niobium benchmark.

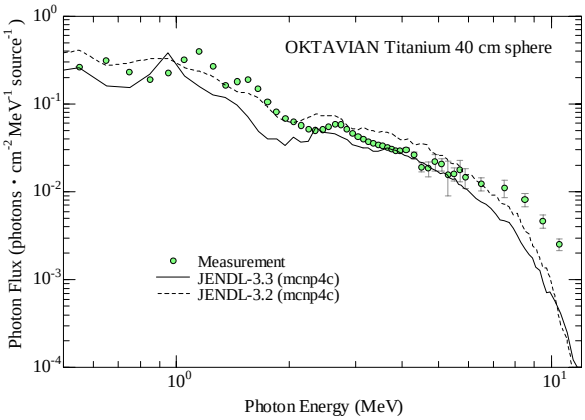

Fig. 21 Results of OKTAVIAN Titanium benchmark.

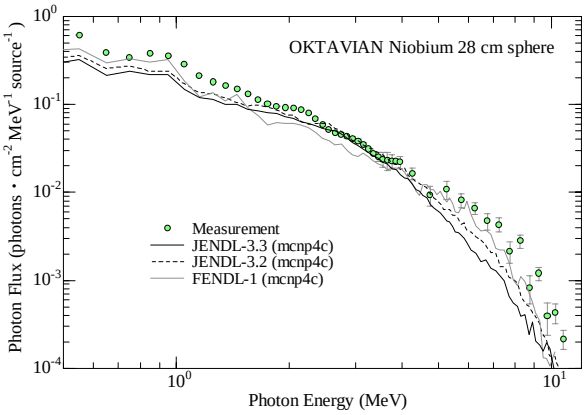

Fig. 22 Results of OKTAVIAN Niobium benchmark.

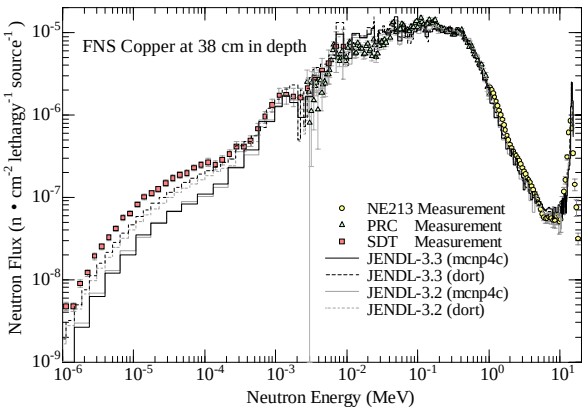

Fig. 23 Results of FNS Copper benchmark.

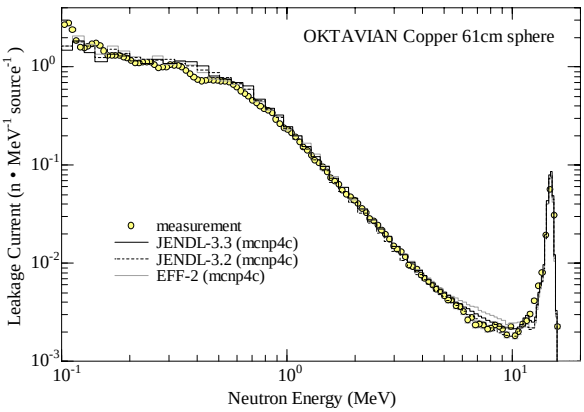

Fig. 24 Results of OKTAVIAN Copper benchmark.